JBC Papers in Press. Published on March 30, 2017 as Manuscript M117.784280
The latest version is at http://www.jbc.org/cgi/doi/10.1074/jbc.M117.784280

Demethylation of Induced Pluripotent Stem Cells from Type 1 Diabetic Patients Enhances Differentiation into Functional Pancreatic β-cells

Gohar S. Manzar*,[1,2,3,4], Eun-Mi Kim*,[1,3,5], and Nicholas Zavazava[1,2,3]
*Equally contributed to this work.

From the [1]Department of Internal Medicine, [2]Department of Biomedical Engineering, University of Iowa, Iowa City, IA, [3]Veterans Affairs Medical Center, Iowa City, IA, [4]Mayo Clinic College of Medicine, Rochester, MN, and [5]Predictive Model Research Center, Korea Institute of Toxicology, Daejeon, Republic of Korea

Running title: T1D patient iPS cell-derived Insulin Producing Cells

To whom correspondence should be addressed: Nicholas Zavazava, M.D., Ph.D. The University of Iowa Hospitals and Clinics, Department of Internal Medicine, Division of Immunology, C429-1 GH, 200 Hawkins Dr., Iowa City, IA, USA – 52242, Phone: (319) 384-6577, Fax: (319) 356-8280, e-mail: *nicholas-zavazava@uiowa.edu*

Keywords: Induced pluripotent stem cell (iPS cell) (iPSC) · Diabetes · Type 1 diabetes · Cell differentiation · Insulin Producing Cells · 3D differentiation · Beta cell (β-cell) · Pancreatic islet

ABSTRACT

Type 1 diabetes (T1D) can be managed by transplanting either the whole pancreas or isolated pancreatic islets. However, cadaveric pancreas is scarcely available for clinical use, limiting this approach. As such, there is a great need to identify alternative sources of clinically usable pancreatic tissues. Here, we used induced pluripotent stem (iPS) cells derived from patients with T1D to generate glucose-responsive, insulin-producing cells (IPCs) via 3D culture. Initially, T1D iPS cells were resistant to differentiation, but transient demethylation treatment significantly enhanced IPC yield. The cells responded to high-glucose stimulation by secreting insulin *in vitro*. The shape, size, and number of their granules, as observed by transmission electron microscopy, were identical to those found in cadaveric β cells. When the IPCs were transplanted into immunodeficient mice that had developed streptozotocin-induced diabetes, they promoted a dramatic decrease in hyperglycemia, causing the mice to become normoglycemic within 28 days. None of the mice died or developed teratomas. Because the cells are derived from "self", immunosuppression is not required, providing a much safer and reliable treatment option for T1D patients. Moreover, these cells can be used for drug screening, thereby accelerating drug discovery. In conclusion, our approach eliminates the need for cadaveric pancreatic tissue.

INTRODUCTION

T1D is a chronic, debilitating autoimmune disease targeting pancreatic β-cells. This process in T1D patients results in a decrease of the pancreatic beta cell mass, which causes insufficient insulin production[1]. The ensuing dysmetabolism leads to serious complications, including cardiovascular disease, diabetic neuropathy, and nephropathy[1]. Although the exact etiology of T1D remains unknown, it is prevalent among young children and remains without a practical cure despite being one of the most common endocrine disorders. Successful transplantation of the pancreas or that of pancreatic islets can prevent or reduce some of the complications of T1D. However, organ shortage severely limits organ transplantation in these patients.

Pluripotent stem cells (PSCs) hold tremendous promise in addressing many of these shortcomings since their availability is unlimited and they are considered to be immune-privileged[2-4]. Both iPS and ES cells are capable of forming any cell type, if provided with appropriate developmental cues[4]. Unlike ES cells that require the controversial destruction of embryos, iPS cells

are derived from pre-existing somatic cells and enable the possibility of designing patient-tailored therapies[4]. These characteristics of iPS cells provide the unique opportunity to engineer autologous IPCs that can be used to replace pancreatic β-cells destroyed in T1D [5]. Moreover, these cells have enormous value in drug screening as well as in modeling the pathogenesis of T1D.

The process of differentiating ES or iPS cells into pancreatic endocrine cells *in vitro* traces the developmental stages observed during embryogenesis[6]. We and others [7-12] have begun to differentiate iPS cells into IPCs. Overall, it has proven challenging to generate mature and functional IPCs that possess hallmark features of adult pancreatic β-cells, such as glucose responsiveness and rapid correction of hyperglycemia[8-12]. More recently, two reports overcame these shortcomings and devised strategies to differentiate human ES and iPS cells into glucose-responsive IPCs that strongly resembled adult pancreatic β-cells[13,14]. Unfortunately, the rate of glucose correction after transplantation of the cells into diabetic mice was 6-7 weeks. Here we show that we can correct hyperglycemia in less than 4 weeks.

We independently overcame the hurdles in the generation of IPCs from human iPS cells by replacing 2D culture platform systems used in prior protocols with a 3D differentiation culture system. The number of IPCs derived was superior to what had been originally described in the literature for traditional 2D culture systems[8-12] and comparable to what has recently been achieved using suspension-based 3D cultures[13,14]. The reason for this improvement is that, during embryogenesis, the developing cells are arranged in 3D clusters, which support cell-cell signaling [15,16]. 3D differentiation of human iPS cells has notable precedent in the literature, having been used to derive functionally and morphologically superior tissues, such as cerebral organoids[15] and liver buds [17]. Here, we established 3D cultures using Matrigel, which is an extracellular matrix-containing rich bioactive substrates, to exploit scaffold-embedded signaling cues [18,19]. By combining a novel 3D bio-scaffold-based culture platform with well-selected and optimized signaling cues, we envisioned that we could drastically improve the efficiency of generating glucose-responsive IPCs.

iPS cells derived from some T1D patients have been shown to have a lower efficiency in generating pancreatic progenitor cells expressing Pdx1[20]. It is not yet known why this is the case, especially since other T1D iPS cell lines have been used to make IPCs efficiently. If this resistance to differentiation is common to a significant number of T1D cell lines, autologous iPS cell therapy for T1D will be a challenge. As a possible way to overcome this, here we show that transient demethylation treatment during the differentiation of a T1D iPS cell line that, in our experience, poorly differentiates into IPCs, can significantly improve the yield of functional IPCs.

RESULTS

Differentiation of T1D and non-diabetic (ND) iPS cells into definitive endodermal (DE) cells

We and others have published preliminary data on the differentiation of iPS cells from healthy individuals[7-14], however the differentiation of iPS cells into IPC has remained elusive. Here, we incorporated additional critical signaling cues that instruct iPS cells to become pancreatic β-cells in order to further improve the yield of IPCs (Fig. 1A). The differentiation process drives the cells through five stages lasting a total of 27 days. The first stage of differentiation towards IPCs is the conversion of iPS cells into definitive endodermal cells (DE cells)[6] after treatment with Activin A and Wnt3a signaling[10] (Stage 1). DE cells are characterized by the expression of CXCR4 and the simultaneous expression of the transcription factor Sox17. The resulting cells are next exposed to FGF-7, which acts to convert the DE cells into the posterior foregut[10] (Stage 2). Following this step, the cells are treated with retinoic acid and SANT-1, an inhibitor of the Shh pathway[10], in order to posteriorize the gut tube and promote pancreatic differentiation as opposed to hepatic specification[21]. Reinforcing suppression of hepatic differentiation, Noggin is added to this media cocktail as well[10]. It functions to inhibit BMP signaling[22]. The aim of this phase is to generate $Pdx1^+$ pancreatic precursor cells (Stage 3). The cells are then instructed to become pancreatic endocrine precursor cells by carrying over certain cues from Stage 3, such as Noggin and low-dose Retinoic Acid signaling, and supplementing them with inhibitors of TGF-β signaling[23] and suppression of Notch signaling[13,14], which actively

inhibit endocrine differentiation by the process of lateral inhibition[24]. Suppression of TGF-β signaling is accomplished by the treatment with ALK5 inhibitor II[25]. Repression of Notch signaling is indirectly accomplished by blockade of its ligand, γ-secretase, using DAPT[26]. In addition, this stage of differentiation introduces several drivers of pancreatic β-cell development, such as thyroid hormone (T3)[13,14] and the incretin GLP-1[27] (Stage 4). Finally, in the last stage of differentiation, specific inducers of insulin are added in addition to agents that promote the maturation and development of pancreatic β-cells, such as nicotinamide[28-30], IGF-1[27,31], GLP-1, and T3.

Using this protocol, ND and T1D iPS cells were first differentiated into DE cells in parallel and the efficacy of differentiation was assessed on day 5 by determining the expression of CXCR4, Sox17, and PDGFR-α. Co-expression of CXCR4 and Sox17 typifies lineage commitment to the endoderm. Undifferentiated iPS cells were utilized as negative controls and did not express any of the aforementioned markers (Fig. 1B). Both T1D-1 and ND differentiated cultures contained >90% $CXCR4^+$ $Sox17^+$ endodermal cells (Fig. 1B). Additionally, these cells were mostly PDGFR-α^- (Fig. 1B), which suggests that they are true endodermal cells and are not arrested in the transitory, immature mesendodermal state[32]. Thus, we concluded that we were able to achieve a near pure population of DE cells from both ND and T1D iPS cells at comparable yields. For further differentiation into IPCs, we dissociated the 2D differentiating DE cells by scraping the monolayers into chunks of cells, and then depositing these cell clusters into matrigel blocks (1:1 diluted with DMEM/F-12). The cells coalesced into discrete spheroids that embedded into the matrigel within 24 h. At this point both cell types were transferred to plates containing matrigel, allowing differentiation of the cells on a 3D platform.

T1D iPS cells predominantly derive hollow cysts that do not express insulin

Early in the 3D differentiation procedure, we recognized that the DE cells from both T1D and ND IPC cultures coalesced into compact cell clusters. However, in the final stage of the differentiation, we observed the formation of clusters with two distinct morphological phenotypes: hollow cysts that appeared like cysts, and compact spheroids (Fig. 1C). Strikingly, we observed that the T1D IPC cultures consisted almost entirely of hollow cysts, whereas the ND iPS cells gave rise to a ratio of 50:50 of hollow cysts to compact spheroids (Fig. 1E). The cysts emerged gradually with the differentiation process, becoming more prominent towards the end of the differentiation. The whole differentiation period lasted 27 days. To further characterize these hollow cysts and compact spheroids, they were stained for insulin. The hollow cysts collapsed upon fixation in paraformaldehyde (Fig. 1D), which is an observation that is consistent with what has been described in the literature with *ex vivo* culture of mouse embryonic pancreatic progenitor cells[33]. When we stained these structures for insulin, the compact spheroids, but not the hollow cysts, stained positive for insulin (Fig. 1D).

Remarkably, the morphology of the compact spheroids resembled that of pancreatic islets (Fig. 1D). This result suggested that in order to optimize the yield of IPCs, the number of the compact spheroids needed to increase.

The differentiation of T1D iPS cells into IPCs has lower efficiency compared to that of ND iPSCs

As determined by flow cytometry, the 25-50.5% yield of IPCs derived from ND iPS cells (across two different iPS cell lines) is comparable to the frequency of β-cells found in primary human islets[34]. This yield of IPCs from ND iPS cells is far superior when compared to previous reports, where the yield of IPCs was only 10-15%[7-12], and is comparable to what was achieved more recently by two groups in 2014 using suspension-based 3D cultures[13,14]. We concluded that 3D differentiation is superior for iPS cell differentiation compared to 2D differentiation. However, despite the effectiveness of our protocol, yield of IPCs from a T1D-1 iPS cell line we possessed was only 15.9%, which was significantly lower than those of ND iPS cells (Fig. 2A and Fig. 4B). Thus, these data allow us to conclude that the differentiation of T1D cell lines into insulin-expressing cells is diminished.

T1D iPS cell-derived differentiating cells poorly express Pdx1

To further investigate why the differentiation of T1D iPS cells was impaired, we next corroborated the immunofluorescence and flow cytometry data by gene expression studies. Gene expression for several genes was studied in Stages 4 and 5 of both T1D and ND differentiation cultures. As can be seen in Fig. 2B, the expression of the *Insulin* transcript in the ND cells increases from Stage 4 to Stage 5, and this is accompanied by a decline in the expression of *Glucagon*, suggesting commitment of the cells toward insulin-expressing cells in the last stage of the differentiation. However, in the T1D IPC differentiating cultures, we observed significantly lower expression of *Insulin* at both Stages 4 and 5, confirming our previous results. We also observed significantly poorer expression of *Glucagon* in the T1D IPC cultures compared to ND IPC cultures. The expression of other genes, such as *Somatostatin* and *Glucokinase* was not significantly different between the T1D-1 and ND cultures, and *Ghrelin* showed a very small but significant difference (Fig. 2B).

To determine if the inefficiency in differentiation manifests earlier than the last stage of differentiation, we determined the expression of *Pdx1* in T1D and ND IPC differentiating cultures. *Pdx1* is the master regulator gene in the pancreas and its expression appears midway through the differentiation process[10]. In ND cultures, *Pdx1* is expressed in high levels in Stage 4 (Fig. 2B), which precedes the expression of *Insulin* in Stage 5, consistent with embryonic development of the pancreas[35]. *Pdx1* levels continue to increase in Stage 5 in the ND culture. However, at both Stages 4 and 5, the T1D-1 cultures expressed significantly lower levels of *Pdx1* than the ND culture (Fig. 2B). Pdx1 is indispensable for the development of pancreatic β-cells[6]. Pdx1 knockout mice fail to form a pancreas[36], which is evidence for how critical this gene is in the development of the pancreas. This likely explains why the expression of downstream genes, such as *Insulin*, is also impaired in the T1D differentiating cultures.

Effective differentiation of T1D iPS cells requires precise temporal modulation of demethylation treatment

We so far demonstrated that the differentiation of T1D iPS into IPCs was impaired for reasons that are still unclear. Considering the importance of epigenetics in cell differentiation and the poor expression of *Pdx1* in T1D differentiating cultures, we hypothesized that epigenetic barriers were likely responsible for the poor yield of IPCs derived from T1D iPS cells. We reasoned that the dysmetabolism in T1D might be responsible for the epigenetic changes which could lead to the poor differentiation of T1D iPS cells. To address this problem, we utilized 5-Aza-2'-deoxycytidine (5-Aza-DC), a potent demethylating agent that inhibits the DNA methyltransferase (Dnmt), thereby inhibiting methyl group deposition on cytosine residues of DNA, including on gene promoters[37]. This allows for the binding of the transcriptional machinery and promotes gene expression. We further argued that the use of a demethylation agent might induce a more labile, permissive state of the stem cells, allowing for greater cell responses to differentiation stimuli, and ultimately enhance the yield of IPCs from T1D iPS cells.

We established a dose-screen experiment to identify the optimal dose of 5-Aza-DC for treatment that would preserve cell viability while effectively demethylating the DNA of the cells. We utilized 1 nM and 10 nM of 5-Aza-DC for our pilot differentiation. To determine the effectiveness of the proposed doses in demethylating iPS cells, we performed a dot blot assay[38] for 5-methylcytosine on genomic DNA isolated from iPS cells that were treated with 1 nM or 10 nM 5-Aza-DC for 18 hours. Untreated iPS cells were used as negative controls. At the 1 nM and 10 nM 5-Aza-DC treatments, we observed loss of methylation in iPS cells as evidenced by the lighter spots on the film, corresponding to lower levels of 5-methylcytosine in these cells (Fig. 2C).

Having confirmed that the doses above resulted in decreased 5-methylcytosine content in the iPS cells, we next sought to optimize the time point for the demethylation. We considered two possible time points for the demethylation treatment: (1) at the start of the differentiation into DE cells, or (2) after the generation of DE cells, before the cells progress into the stage in which $Pdx1^+$ cells are generated. We observed that the treatment of iPS cells with 10 nM 5-Aza-DC on day 0 of differentiation (before initiating the generation of DE cells) resulted in cells on day 5

that were arrested in the immature CXCR4$^+$ PDGFRα$^+$ Sox17$^-$ mesendodermal state (Fig. 3A). In contrast, demethylation of the cells on day 4 of differentiation, which is the day when DE cells are harvested, yielded a pure population of CXCR4$^+$ Sox17$^+$ PDGFRα$^-$ DE cells, similar to what we were able to generate without any demethylation agent. This pilot experiment allowed us to conclude that the 5-Aza-DC treatment was ideal after the generation of DE cells.

Demethylation of T1D DE cells rescues the expression of Pdx1 and leads to the generation of islet-like compact cell clusters

After identifying the appropriate doses and time point at which demethylation would be implemented, we initiated a full differentiation of T1D iPS cells into IPCs, demethylating the DE cells on day 4 for 18 hours before transferring them onto matrigel. We observed a striking impact of the 5-Aza-DC treatment in the T1D cultures. Typically, the T1D iPS cells we possessed gave rise to a disorganized mix of cysts and spheroids, with a dominant presence of hollow cysts. At both doses tested, 5-Aza-DC treatment instead promoted the formation of compact cell clusters (Fig. 3B). Juxtaposition of the clusters derived from the two treatment conditions showed that regardless of the dose, demethylation generated cell clusters that uniquely resembled human islets (Fig. 3B). Next, we stained these cell clusters with dithizone, which is an organic compound that complexes with Zn^{2+} ions found in insulin hexamers of β-cell insulin granules, and thus suggests the presence of insulin [39]. Dithizone staining revealed the strong red color of the compact clusters found in the 1 nM and 10 nM 5-Aza-DC treated cultures, which was reminiscent of islets (Fig. 3B). This was in contrast to what was observed in the IPCs derived from untreated iPS cells, which stained brown in a manner similar to undifferentiated iPS cells (Fig. 3B).

Next, we assessed whether the demethylation rescued the expression of Pdx1 in the differentiating T1D IPC cultures. We chose to address this question by determining the expression of Pdx1 in the differentiating cells using flow cytometry. Undifferentiated iPS cells were used as negative controls in these experiments (Fig. 3C), and the mouse insulinoma βTC3 or human cadaveric β-cells served as positive controls (Fig. 3C)

As described above, without the demethylation step, the yield of insulin-expressing cells from T1D iPS cells was lower than ND iPS cells (Fig. 2A), which is consistent with the 12% yield of Pdx1$^+$ pancreatic progenitor cells observed in regular differentiations at the end of Stage 4 (Fig. 3C). However, after demethylation, we observed robust expression of Pdx1 (~95%) at the end of Stage 4 (Fig. 3C). Curiously, demethylation of differentiating ND cells did not significantly improve the yield of Pdx1$^+$ cells. 71.1% of the non-demethylated cells expressed Pdx1 compared to 76.1% after demethylation (Fig. 3C). In T1D differentiating cultures, a significant proportion of cells co-expressed Pdx1 and the pancreatic β-cell specific transcription factor Nkx6.1, which is critical for maintaining the identity and function of pancreatic β-cells[40,41] (Fig. 3D). Altogether, these data suggested that the transient demethylation treatment allowed the expression of Pdx1 in differentiating T1D cultures.

Demethylation of T1D DE cells significantly improves the differentiation of DE cells into pancreatic cells

These data then led us to wonder if 5-Aza-DC treatment enhanced the expression of downstream targets of Pdx1, such as insulin[42], and made the cells more receptive to differentiation cues while averting commitment towards alternative lineages. For this experiment, we were able to obtain a separate T1D iPS cell line, which also showed resistance to differentiating into IPCs. As can be seen in Fig. 4A, demethylation improved the yield of IPCs from 13.7% to 56.7% in T1D-1 and from 1% to 59.4 % in T1D-2, which was very similar to human islets (58.4%). T1D-1 iPS cells were assessed for insulin expression as a negative control. Notably, the yield of IPCs from ND iPS cells was not changed even after 5-Aza-DC treatment (Fig. 4B).

A key sign of the efficiency of the differentiation is the relative ratio of β-cells versus α-cells. Specifically, we sought to determine the proportion of IPCs relative to those that stain for glucagon. Most reports published so far generate multihormonal cultures that express both insulin and glucagon[7-12]. As can be seen in Fig. 4C, the proportion of glucagon-expressing cells was quite

high when the iPS cells were not demethylated, whereas they were depleted after the demethylation step (Fig. 4C). Non-demethylated cultures yielded up to 13% insulin-expressing cells and 50% glucagon-producing cells. However, with demethylation at a dose of 10 nM 5-Aza-DC, 56% of the cells expressed insulin, with a much smaller portion of the cells expressing glucagon, Fig. 4C. This result also demonstrates that, at higher concentrations of the demethylating agent, nearly all the glucagon secreting cells are gone. Because the highest yield resulted from treatment of the cells with 10 nM 5-Aza-DC, we chose to use this dose for all subsequent experiments. This experiment has been repeated multiple times and as many as 65% insulin^{+} cells were measured in some cultures. Pooling of data from several differentiations reveals that 5-Aza-DC treatment consistently enhances the yield of IPCs 4-fold (Fig. 4D).

T1D IPCs derived from demethylated DE cells express pancreatic β cell-specific markers and possess insulin granules at similar levels to cadaveric β-cells

Until very recently, mainstream published protocols for the generation of IPCs from iPS or ES cells generally give rise to a multihormonal pool of cells, of which very few cells express only insulin[7-12]. We showed so far that our newly established protocol allowed for the selective generation of insulin-expressing cells from T1D iPS cells while generating very few glucagon-expressing cells. Immunofluorescence analysis of the differentiated cell clusters showed that the cells were mostly insulin secreting cells only with a very small percentage of glucagon secreting cells (Fig. 5A). Thus, demethylation appears to promote the generation of monohormonal insulin-expressing cells while averting the formation of glucagon-producing cells.

Additionally, we stained for the nuclear transcription factor Nkx6.1, which is critical for the maintenance of pancreatic β-cell function and identity[40,41]. The cells were co-stained for the insulin precursor C-peptide, which is synonymous with *de novo* production of insulin[27,43]. As evidenced in Fig. 5B, T1D IPCs derived via demethylation show robust expression of C-peptide in the cytoplasm as well as strong nuclear expression of Nkx6.1 (Fig. 5B). This confirms the flow cytometry results for Nkx6.1 (Fig. 3D) and affirms our conviction that we have established a protocol that efficiently generates IPCs.

Next, we analyzed the ultrastructure of these cells by Transmission Electron Microscopy (TEM). We observed a unique pancreatic β-cell like morphology of the granules contained in the T1D IPCs (Fig. 5C, bottom panel). Unlike our first protocol that was recently published[7], these granules are identical to those present in cadaveric β-cells (Fig. 5C, top panel). Insulin granules undergo various stages of maturation that are differentiated by the shape and darkness of the core[13,14]. The most mature insulin granules are angular due to the hexamer complexation of insulin with zinc, which creates a crystalline shape[44]. However, insulin granules universally possess a characteristic "halo" (which is an artifact of the gluteraldehyde fixation) that is not found on any other hormone granule[44]. This feature is thus a unique and specific indication of β-cell like phenotype.

As can be seen in the lower panel of Fig. 5C, IPCs resemble pancreatic β-cells in their possession of the three different insulin granule subtypes, all of which have the characteristic halo surrounding them. Additionally, the number of granules found in the IPCs was not statistically different from the number of granules in primary human islets (Fig. 5D). Thus, we have generated human IPCs from T1D iPS cells that strongly resemble human β-cells in their ultrastructure in addition to their expression of insulin and other pancreatic β-cell specific markers.

T1D IPCs are functional and are glucose-responsive

Until now, we argued that demethylation promoted the selective generation of insulin-producing cells which are bound in tight cell clusters that strongly resemble islets. Perhaps the most important criterion for defining the authenticity of the generated IPCs is to observe whether they secrete insulin when stimulated with high glucose[45]. This is important since these cells should respond to glucose spikes *in vivo* caused by food intake. Besides, pluripotent stem cell-generated IPCs have failed to respond to glucose stimulation until very recently. Two recent reports described for the first time the generation of glucose-responsive cells from human ES cells[13,14].

Maehr et al, reported the generation of pluripotent stem cells from patients with type 1diabetes and analyzed phenotype of the IPCs[46]. However as of yet, the generation of functional, glucose-responsive IPCs from human iPS cells of T1D patients has not been demonstrated.

To address the glucose-responsiveness of these IPCs, we subjected T1D IPC cell clusters to a glucose stimulated insulin secretion (GSIS) assay, which involves exposing cells sequentially to low glucose (2.8 mM) and subsequently to high glucose (28 mM). Insulin content in the supernatants was measured by ELISA. While the absolute content of insulin produced, when normalized by total protein, was significantly lower for IPCs (2 µIU/mL) than islets (250 µIU/mL) (Fig. 5E and 5F), the fold-increase in insulin production by IPCs is higher than that for islets (Fig.5G). As evidenced in Fig. 5G, these IPCs are glucose-responsive in a manner that has never been observed before in IPCs derived from T1D iPS cells. This result demonstrates the generation of functional IPCs from human iPS cells derived from T1D patients.

Human iPS cell-derived IPCs rapidly correct hyperglycemia in diabetic mice

To determine whether the T1D IPCs are functional *in vivo*, immunodeficient Rag2$^{-/-}\gamma_c^{-/-}$ mice were made diabetic by multiple low doses of STZ. Mice were injected s.c. with 1.2-1.4 x 10^6 of 5-Aza-DC treated T1D-1 iPS cells-derived IPCs in the shoulder region. Remarkably, the hyperglycemia plateaued in less than 2 weeks after transplantation and started to rapidly fall. Within 4 weeks, mice were either normoglycemic or achieved near normoglycemia. None of the 8 mice died or developed teratomas, Fig. 6A. All mice normalized blood glucose levels. Additionally, we subjected mice that showed stable correction of hyperglycemia to a glucose tolerance test (n=4), in which they received a supraphysiological glucose bolus i.p. The management of this glucose spike was then assessed over a period of time in order to determine the kinetics of blood glucose regulation. Remarkably, in contrast to non-transplanted diabetic mice, which failed to correct hyperglycemia, and were ultimately sacrificed, IPC-transplanted mice completely recovered to normoglycemia in 4 hours (Fig. 6B). This is evidence for how the IPCs endowed these formerly diabetic mice with the ability to tolerate and manage glucose spikes. However, we noted that the correction of hyperglycemia was significantly delayed compared to nondiabetic control mice, suggesting that there is a need for further improvement. Perhaps increasing the cell numbers might speed up the recovery from the glucose bolus levels. Still, the complete return to normoglycemia in IPC-transplanted mice is striking evidence of the remarkable ability of these cells to manage supra-physiological glucose spikes. Excision of the transplanted cells after 8 weeks of s.c. transplantation revealed an organoid (Fig. 7A) that showed glandular morphology of cells surrounded by adipocytes and the presence of duct-like lumens, evidenced by H&E staining (Fig. 7B). The morphology of these cells was highly similar to H&E staining in 10 week old organoids when IPCs were transplanted under the kidney capsules[14]. Interestingly we identified by immunofluorescence parts of the organoid that stained positive for insulin only (Fig. 7C), and other areas that expressed both insulin and somatostatin (Fig. 7D). Glucagon staining remained negative. Thus, T1D IPCs differentiated through this protocol generate vascularized organoids that consist of insulin- and somatostatin-expressing cells after transplantation into mice.

DISCUSSION

Our data demonstrate that we have established a robust protocol for the generation of IPCs from either healthy or T1D iPS cells. These findings align with recent reports[13,14] that utilize different 3D differentiation methods that altogether have facilitated an enormous advance from prior protocols that generally yielded only 10-15% insulin$^+$ cells from human ES cells or iPS cells derived from nondiabetic patients[7-12]. Our protocol is simple, reproducible and does not require exorbitant amounts of expensive reagents and growth factors. Here, we utilized a highly optimized system to generate a virtually pure population of CXCR4$^+$ Sox17$^+$ DE cells that did not express PDGFR-α, a mesodermal and mesendodermal marker [32]. These cells were then driven through four more developmental stages in a 3D platform to yield >50% insulin$^+$ IPCs. These cells were organized in compact cell clusters that resemble islets and expressed insulin as determined by a glucose stimulation assay, flow

cytometry, qRT-PCR, and immunofluorescence. Although we detected some somatostatin expressing cells and insulin producing cells, glucagon was not detectable.

However, the success of this protocol in yielding IPCs from ND iPS cells was clearly not recapitulated in two T1D iPS cells we possessed. Although the early differentiation of T1D and ND iPS cells into DE cells (Stage 1) was equivalent, downstream 3D differentiation of the iPS cells showed striking disparities between the two cell types. This was first observed in morphological differences between T1D and ND IPC differentiating cultures, whereby the T1D IPC culture yielded 85% insulin-negative hollow cysts and 15% insulin-expressing compact clusters, but the ND culture gave rise to a 50:50 mixture of the two cluster types (Fig. 1E). Interestingly, these hollow cysts have been observed by another group that differentiated human ES cells into islet-like clusters dishes[47].

Our observation of the dichotomy in cluster types is consistent with data that was presented in a manuscript that reported the use of growth-factor depleted Matrigel to expand mouse embryonic pancreatic progenitor cells[33]. Depending on their medium, that group was able to derive two discrete sets of cell clusters. In one form of media, pancreatic progenitors underwent differentiation *in vitro* into complex organoids consisting of mature pancreatic endocrine, acinar and ductal cells. However, a different set of media sustained pancreatic progenitors that assembled into hollow spheres, which consisted of cells that had not differentiated into mature pancreatic cells. Correlating these findings with our own data, this alludes to a bivalent state for the clusters in our differentiating cultures, which consist of compact spheroids that contain mature IPCs and express insulin, as well as hollow, vacuolar cysts that contain immature progenitor cells that do not yet express insulin. Significantly, the dominant presence of hollow cysts in the T1D IPC cultures suggested that most of the cells were immature and that their normal development into IPCs was impaired.

Indeed, as determined through several parameters, we have shown that the generation of insulin-expressing cells from two T1D iPS cell lines in our possession is impaired. Tracing the disparity in the differentiations backward to earlier in the pancreatic differentiation program revealed that the expression of the *Pdx1* transcript was extremely poor in T1D iPS cell differentiating cultures, suggesting that the differentiation of T1D DE cells into $Pdx1^+$ pancreatic progenitor cells was impaired. Naturally, this would translate into significantly impaired yield of insulin-expressing IPCs at the end of the differentiation. Thus, we conclude from these data that the differentiation of some T1D iPS cells into IPCs is impaired compared to ND iPS cells. This could be due to variability between different iPS cell lines. However, the Melton group also showed poor differentiation of one T1D cell line in their possession, suggesting that this phenomenon may be worth investigating in larger panels of T1D iPS cell lines. Indeed, our findings are consistent with their utilization of T1D iPS cells as a negative control for generating $Pdx1^+$ pancreatic progenitor cells[20]. Whereas that study stopped differentiating cells at Stage 3, our studies advance several steps ahead of this report since we compared the differentiation of ND and T1D iPS cells all the way to Stage 5 using a robust 3D differentiation protocol. Additionally, whereas that prior report briefly introduced their finding, here we have devised a protocol that overcomes this hurdle and allows for robust differentiation of resistant human T1D iPS cells into functional, therapeutic IPCs that respond to high glucose stimulation.

After obtaining the gene expression data showing the impaired expression of the *Pdx1* mRNA transcript in T1D differentiating cells, we reasoned that there were epigenetic barriers that hindered the expression of critical genes for pancreatic β-cell specification, such as *Pdx1*. Thus, we hypothesized that using epigenetic modifiers such as 5-Aza-DC would allow for the expression of *Pdx1* and downstream genes, which altogether would ultimately improve the differentiation outcome and result in a high yield of $insulin^+$ IPCs from resistant T1D iPS cells.

Following this hypothesis, we thus treated the T1D culture with 5-Aza-DC after the generation of DE cells, which is the time point after which impaired differentiation is observed. Treatment of iPS cells with 5-Aza-DC yielded >95% $Pdx1^+$ pancreatic progenitor cells from T1D iPS cells at the end of Stage 4, which eventually gave rise to >50% insulin-expressing IPCs organized into compact, islet-like clusters. This

yield is comparable to what we observed in human islets and in ND IPCs differentiating cultures. When we determined the proportion of insulin-expressing cells versus glucagon-expressing cells in the cultures, we found that 5-Aza-DC improved the yield of IPCs in a concentration-dependent manner while averting the generation of glucagon-expressing cells. This suggested that demethylation was making the differentiating cells more receptive to pancreatic differentiation cues. This specific but still unexplored mechanistic role of 5-Aza-DC in enhancing the differentiation of T1D iPS cells into IPCs strongly suggests a metabolic, inflammatory, or other cause of epigenetic variability in those cells versus ND cells at the level of methylases, methyltransferrases, or methylation patterns. This gap in the mechanistic understanding of our findings demands further investigation. Additionally, we arrived at our choice of demethylation agent by serendipity and without specific evidence that it would upregulate the expression of *Pdx1*. We also appreciate that 5-Aza DC may not be the ideal demethylating agent because it could lead to DNA damage. Altogether, these facts embolden the need to investigate other demethylation agents in the future.

Further characterization of these cells showed that IPCs possessed insulin granules and had the capability for GSIS. However, we found that glucose- and KCL-responsive insulin secretion by the IPCs still remained 1/100 to 1/125th of human islets (Fig. 5E and F). If not an issue of insulin content, our findings could be explained by a secretory defect in the IPCs that should be identified and corrected. This raises questions about the need for the *in vivo* microenvironment before the cells fully mature. Whether this significant difference between IPCs and native islets is due to decreased insulin content or impaired secretion of insulin is still unclear. Indeed, a limitation of this study is that we have not fully developed an understanding of the insulin content and biosynthesis machinery of iPS cell-derived IPCs compared to islets from a true quantitative standpoint. Our use of TEM in Fig. 5 is much more robust in allowing us to make qualitative conclusions. The number of granules is not a suitable surrogate for cellular insulin content and so we would need to address this question further in future studies.

Nonetheless, confirmation that our cells are true β-cells came from the transplantation data, which show very rapid correction of hyperglycemia in diabetic mice. In comparison to most other data published by others, our cells abrogate the rise in hyperglycemia and rapidly induce normoglycemia in 4 weeks. In a clinical situation, this would be highly desirable. Additionally, we showed through a glucose tolerance test that IPC-transplanted mice were able to effectively manage a supraphysiological glucose load, returning to baseline normoglycemia after four hours, whereas nontransplanted diabetic counterparts remained hyperglycemic. Importantly, however, we observed a striking delay in the correction of hyperglycemia in IPC-transplanted mice compared to nondiabetic, healthy mice. While we did not collect data on the kinetics of human insulin secretion in these mice during the procedure, we speculate that this markedly slowed return to normoglycemia is due to impaired insulin secretion in IPCs compared to native islets, which is a phenomenon that further bolsters the need for deeper analysis.

One other remarkable finding in our study is that it appears that the location of the transplanted cells in the recipient mice does not matter. In a previous report, we transplanted the cells under the kidney capsule, where the cells induced neovascularization and corrected hyperglycemia[7]. Because the kidney capsule can maintain the cells in one spot, we were able to harvest a much larger organoid after 3 months. Here, we probed another site, namely the subcutaneous space on the shoulder flank as published by others[38], which is why the cells are embedded in adipocytes. The rationale for doing this is that the skin is highly vascularized and the procedure is simpler than the major surgery that is involved in subcapsular kidney transplantation. We do not attribute differences in the speed by which normalization of the glucose levels occurred or in the degree by which correction happened to the injection site but instead to the maturity of the cells. Clearly, the cells generated through our latest protocol were significantly more mature than our prior report, as demonstrated by the greater number of granules and the superior speed with which they corrected hyperglycemia. Interestingly, the IPCs were surrounded by adipocytes, which is consistent with the observation that insulin

promotes adipocyte growth[48]. Lastly, none of the mice developed teratomas. Thus, our data show rapid correction of hyperglycemia in diabetic mice using IPCs derived from T1D human iPS cells. Notably, we explored if removal of the graft resulted in hyperglycemia. While it did lead to a significant rise in blood glucose levels (data not shown), overt hyperglycemia (>250 mg/dL) was not seen. This is likely because because graft excision was not guaranteed considering the original subcutaneous injection of the cells. This is a drawback of this method as opposed to injecting the cells under the kidney capsule.

Our findings are highly significant since iPS cell-based therapy for T1D will, in all likelihood, involve the patient's own somatic cell-derived iPS cells[4,5]. With most prior reports using human ES cells or iPS cells derived from health subjects[7-12], we expect more studies to better understand the influence of T1D on the differentiation of iPS cells derived from individuals suffering from T1D. Indeed, our studies underscore the need to address inadequacies in the differentiation of some T1D iPS cell lines into IPCs before such therapy is hastily translated into the clinic. Here, we demonstrate a highly efficient protocol for using demethylation as a strategy to induce directed derivation of IPCs from resistant T1D patient-derived iPS cells. The success of a model in which iPS cells will one day be generated from T1D patients and used to generate IPCs will be highly dependent on the results of our current studies, which we hope one day to advance into the clinical realm.

EXPERIMENTAL PROCEDURES

Differentiation of iPS cells into IPCs

To initiate the differentiation of iPS cells into definitive endoderm (DE) cells, they were first maintained in the STEMdiff Definitive Endoderm Kit (Catalog Number: 05110, Vancouver, BC) for 5 days, while cultured on feeder cells as colonies. On day 5, expression of DE cell markers, such as CXCR4 and Sox17, was assessed on these cells to ensure that differentiation was proceeding properly. After confirmation that the culture contained >90% $CXCR4^{+}Sox17^{+}$ cells, the rest of the DE cells were harvested and 3D differentiation was initiated with Media 2. If demethylation of the cells was performed, this was done according to details provided in the Supplementary Information. On the day of 3D differentiation (D5), a 1:1 (vol/vol) mixture of liquid human ESC-qualified matrigel (Catalog Number: 354277, Corning Inc., Tewksbury MA) was mixed with cold DMEM/F-12 in a chilled conical tube. Then, in a 24 well plate, 100 µL of the 1:1 mixture was deposited in the center of each well and the plate was incubated at 37°C for 5 minutes. When a rigid dome had formed in the center of each well, 400 µL of the 1:1 mixture was added on top of this dome and the plate was shaken to allow the matrigel mixture to spread evenly, resulting in a 500 µL layer of matrigel in each well. The plate was replaced at 37°C for 3 hours to allow the matrigel to solidify sufficiently.

2.5 hours into the incubation, the DE cells were harvested and suspended in warm Media 2, which contains Y27632, a ROCK inhibitor intended to promote cell survival. This cell suspension ($2.5\text{-}5X10^{6}$ /well) was distributed on top of the matrigel, with each well thus containing 500 µL of the matrigel mixture and 500 µL of the cell suspension. Generally, within the first 24 hours, most of the DE cell clusters embed into the matrigel scaffold, forming sphere-like clusters at varying depths in the matrigel layer. The plate was left undisturbed for 24 hours, at which point, the first media change in 3D culture was performed as following protocol (Supplementary Table S1).

Glucose stimulated insulin secretion (GSIS) assay

We performed static glucose stimulated insulin secretion (GSIS) assays in order to determine the glucose-responsiveness of IPC clusters (Day 27-30 of culture) as compared to human islets (supplied by the IIDP). We followed standard IIDP standard operating procedures to perform the GSIS assays (detailed in Supplementary Information), and utilized the Human Ultrasensitive Insulin ELISA (Catalog Number: 80-INSHUU-E01.1, ALPCO Diagnostics, Salem, NH) according to manufacturer's instructions for quantitation of insulin levels in the supernatant of these samples. The amount of insulin produced was normalized by the total protein in each sample, which was calculated via the Bradford Assay of the lysate generated from the cell clusters.

Mice and transplantation

All animal procedures were approved by the Institutional Animal Care and Use Committee (IACUC) at the University of Iowa and the Iowa City VA Medical Center, and procedures were conducted in accordance with NIH guidelines. Other detail materials and methods provided in the *Supplementary Information*.

ACKNOWLEDGEMENTS

This work was made possible by support from a VA Merit Award and by the NIH/NHLBI grant 5R01HL073015-08, as well as by funding from ReproCELL Inc. Dr. Kim is supported by an AHA Career Development Award (14SDG18690008). Dr. Manzar was supported by an AAI Careers in Immunology Fellowship Award. We also thank the Integrated Islet Distribution Program (IIDP), City of Hope, Ca, for providing us with cadaveric islets used as positive controls for this study. We would like to thank Pavana Rotti for her help in producing some of the immunofluorescence data in this manuscript. Finally, we would like to acknowledge the Central Microscopy Research Facility (and specifically, Dr. Chantal Allamargot) for her help in generating the TEM data.

COFLICT OF INTEREST

The authors declare no competing financial interests.

AUTHOR CONTRIBUTIONS

G.M., E.M.K., and N.Z. designed the experiments. G.M. and N.Z. wrote the manuscript. G.M. and E.M.K. performed most experiments with the help of N.Z. All authors discussed the results and commented on the manuscript.

REFERENCES

1. Leroux, C., *et al.* Lifestyle and Cardiometabolic Risk in Adults with Type 1 Diabetes: A Review. *Can J Diabetes* **38**, 62-69 (2014).
2. Drukker, M., *et al.* Characterization of the expression of MHC proteins in human embryonic stem cells. *Proceedings of the National Academy of Sciences of the United States of America* **99**, 9864-9869 (2002).
3. Kim, E.M., Manzar, G. & Zavazava, N. Human iPS cell-derived hematopoietic progenitor cells induce T-cell anergy in in vitro-generated alloreactive CD8(+) T cells. *Blood* **121**, 5167-5175 (2013).
4. Robinton, D.A. & Daley, G.Q. The promise of induced pluripotent stem cells in research and therapy. *Nature* **481**, 295-305 (2012).
5. Manzar, G.S., Kim, E.M., Rotti, P. & Zavazava, N. Skin deep: from dermal fibroblasts to pancreatic beta cells. *Immunol Res* (2014).
6. Spence, J.R. & Wells, J.M. Translational embryology: using embryonic principles to generate pancreatic endocrine cells from embryonic stem cells. *Developmental dynamics : an official publication of the American Association of Anatomists* **236**, 3218-3227 (2007).
7. Raikwar, S.P., *et al.* Human iPS cell-derived insulin producing cells form vascularized organoids under the kidney capsules of diabetic mice. *PLoS One* **10**, e0116582 (2015).
8. D'Amour, K.A., *et al.* Production of pancreatic hormone-expressing endocrine cells from human embryonic stem cells. *Nature biotechnology* **24**, 1392-1401 (2006).
9. Kroon, E., *et al.* Pancreatic endoderm derived from human embryonic stem cells generates glucose-responsive insulin-secreting cells in vivo. *Nature biotechnology* **26**, 443-452 (2008).
10. Rezania, A., *et al.* Maturation of Human Embryonic Stem Cell–Derived Pancreatic Progenitors Into Functional Islets Capable of Treating Pre-existing Diabetes in Mice. *Diabetes* **61**, 2016-2029 (2012).
11. Xie, R., *et al.* Dynamic chromatin remodeling mediated by polycomb proteins orchestrates pancreatic differentiation of human embryonic stem cells. *Cell stem cell* **12**, 224-237 (2013).

12. Zhang, D., *et al.* Highly efficient differentiation of human ES cells and iPS cells into mature pancreatic insulin-producing cells. *Cell research* **19**, 429-438 (2009).
13. Pagliuca, F.W., *et al.* Generation of functional human pancreatic beta cells in vitro. *Cell* **159**, 428-439 (2014).
14. Rezania, A., *et al.* Reversal of diabetes with insulin-producing cells derived in vitro from human pluripotent stem cells. *Nat Biotechnol* **32**, 1121-1133 (2014).
15. Lancaster, M.A., *et al.* Cerebral organoids model human brain development and microcephaly. *Nature* **501**, 373-379 (2013).
16. Takebe, T., *et al.* Vascularized and functional human liver from an iPSC-derived organ bud transplant. *Nature* **499**, 481-484 (2013).
17. Takebe, T., *et al.* Generation of a vascularized and functional human liver from an iPSC-derived organ bud transplant. *Nat. Protocols* **9**, 396-409 (2014).
18. Hughes, C.S., Postovit, L.M. & Lajoie, G.A. Matrigel: a complex protein mixture required for optimal growth of cell culture. *Proteomics* **10**, 1886-1890 (2010).
19. Kleinman, H.K. & Martin, G.R. Matrigel: basement membrane matrix with biological activity. *Semin Cancer Biol* **15**, 378-386 (2005).
20. Chetty, S., *et al.* A simple tool to improve pluripotent stem cell differentiation. *Nature methods* **10**, 553-556 (2013).
21. Mfopou, J.K., Chen, B., Sui, L., Sermon, K. & Bouwens, L. Recent advances and prospects in the differentiation of pancreatic cells from human embryonic stem cells. *Diabetes* **59**, 2094-2101 (2010).
22. Groppe, J., *et al.* Structural basis of BMP signalling inhibition by the cystine knot protein Noggin. *Nature* **420**, 636-642 (2002).
23. Loh, K.M., *et al.* Efficient endoderm induction from human pluripotent stem cells by logically directing signals controlling lineage bifurcations. *Cell stem cell* **14**, 237-252 (2014).
24. Murtaugh, L.C., Stanger, B.Z., Kwan, K.M. & Melton, D.A. Notch signaling controls multiple steps of pancreatic differentiation. *Proceedings of the National Academy of Sciences of the United States of America* **100**, 14920-14925 (2003).
25. Gellibert, F., *et al.* Identification of 1,5-naphthyridine derivatives as a novel series of potent and selective TGF-beta type I receptor inhibitors. *Journal of medicinal chemistry* **47**, 4494-4506 (2004).
26. Firth, A.L., *et al.* Generation of multiciliated cells in functional airway epithelia from human induced pluripotent stem cells. *Proceedings of the National Academy of Sciences of the United States of America* **111**, E1723-1730 (2014).
27. Thatava, T., *et al.* Indolactam V/GLP-1-mediated differentiation of human iPS cells into glucose-responsive insulin-secreting progeny. *Gene therapy* **18**, 283-293 (2011).
28. Otonkoski, T., Beattie, G.M., Mally, M.I., Ricordi, C. & Hayek, A. Nicotinamide is a potent inducer of endocrine differentiation in cultured human fetal pancreatic cells. *The Journal of clinical investigation* **92**, 1459-1466 (1993).
29. Shahjalal, H.M., *et al.* Generation of insulin-producing beta-like cells from human iPS cells in a defined and completely xeno-free culture system. *J Mol Cell Biol* (2014).
30. Ye, D.Z., Tai, M.H., Linning, K.D., Szabo, C. & Olson, L.K. MafA expression and insulin promoter activity are induced by nicotinamide and related compounds in INS-1 pancreatic beta-cells. *Diabetes* **55**, 742-750 (2006).
31. Withers, D.J., *et al.* Irs-2 coordinates Igf-1 receptor-mediated beta-cell development and peripheral insulin signalling. *Nature genetics* **23**, 32-40 (1999).
32. Tada, S., *et al.* Characterization of mesendoderm: a diverging point of the definitive endoderm and mesoderm in embryonic stem cell differentiation culture. *Development (Cambridge, England)* **132**, 4363-4374 (2005).
33. Greggio, C., *et al.* Artificial three-dimensional niches deconstruct pancreas development in vitro. *Development (Cambridge, England)* **140**, 4452-4462 (2013).

34. Brissova, M., *et al.* Assessment of human pancreatic islet architecture and composition by laser scanning confocal microscopy. *J Histochem Cytochem* **53**, 1087-1097 (2005).
35. Parnaud, G., *et al.* Blockade of beta1 integrin-laminin-5 interaction affects spreading and insulin secretion of rat beta-cells attached on extracellular matrix. *Diabetes* **55**, 1413-1420 (2006).
36. Stoffers, D.A., Zinkin, N.T., Stanojevic, V., Clarke, W.L. & Habener, J.F. Pancreatic agenesis attributable to a single nucleotide deletion in the human IPF1 gene coding sequence. *Nature genetics* **15**, 106-110 (1997).
37. Christman, J.K. 5-Azacytidine and 5-aza-2'-deoxycytidine as inhibitors of DNA methylation: mechanistic studies and their implications for cancer therapy. *Oncogene* **21**, 5483-5495 (2002).
38. Pennarossa, G., *et al.* Brief demethylation step allows the conversion of adult human skin fibroblasts into insulin-secreting cells. *Proceedings of the National Academy of Sciences of the United States of America* **110**, 8948-8953 (2013).
39. Shiroi, A., *et al.* Identification of insulin-producing cells derived from embryonic stem cells by zinc-chelating dithizone. *Stem cells* **20**, 284-292 (2002).
40. Schaffer, A.E., *et al.* Nkx6.1 controls a gene regulatory network required for establishing and maintaining pancreatic Beta cell identity. *PLoS genetics* **9**, e1003274 (2013).
41. Taylor, B.L., Liu, F.F. & Sander, M. Nkx6.1 is essential for maintaining the functional state of pancreatic beta cells. *Cell reports* **4**, 1262-1275 (2013).
42. Murtaugh, L.C. Pancreas and beta-cell development: from the actual to the possible. *Development (Cambridge, England)* **134**, 427-438 (2007).
43. Chen, A.E., Borowiak, M., Sherwood, R.I., Kweudjeu, A. & Melton, D.A. Functional evaluation of ES cell-derived endodermal populations reveals differences between Nodal and Activin A-guided differentiation. *Development (Cambridge, England)* **140**, 675-686 (2013).
44. Norris, D.O. & Carr, J.A. Chapter 12 - Chemical Regulation of Feeding, Digestion and Metabolism. in *Vertebrate Endocrinology (Fifth Edition)* (ed. Carr, D.O.N.A.) 443-481 (Academic Press, San Diego, 2013).
45. Yechoor, V. & Chan, L. Minireview: beta-cell replacement therapy for diabetes in the 21st century: manipulation of cell fate by directed differentiation. *Molecular endocrinology* **24**, 1501-1511 (2010).
46. Maehr, R., *et al.* Generation of pluripotent stem cells from patients with type 1 diabetes. *Proceedings of the National Academy of Sciences of the United States of America* **106**, 15768-15773 (2009).
47. Bose, B., Shenoy, S.P., Konda, S. & Wangikar, P. Human embryonic stem cell differentiation into insulin secreting beta-cells for diabetes. *Cell biology international* **36**, 1013-1020 (2012).
48. Dimitriadis, G., Mitrou, P., Lambadiari, V., Maratou, E. & Raptis, S.A. Insulin effects in muscle and adipose tissue. *Diabetes Research and Clinical Practice* **93, Supplement 1**, S52-S59 (2011).

FIGURE LEGENDS

Figure 1. Solid spheroids but not hollow cysts found predominantly in T1D differentiating cultures express insulin.
A) This differentiation schema shows in a clockwise manner the five stages of differentiation that iPS cells undergo in order to become IPCs.
B) T1D-1 and ND iPS cells were differentiated in parallel under Stage 1 to generate $CXCR4^+$ $Sox17^+$ PDGFR-α^- DE cells. Over 90% of the resultant cells derived from both T1D and ND iPS cells co-expressed CXCR4 and Sox17, and almost all of these cells were PDGFR-α^-, suggesting that they are endodermal but not mesendodermal. Undifferentiated iPS cells were used as negative controls for these stains.

C) The parallel differentiation of T1D-1 and ND iPS cells in 3D culture after Stage 1 results in distinct morphologies of hollow cyst-like (asterisk) and compact (arrowheads) IPC clusters towards the end of the differentiation. Scale bar = 100 μm.
D) Brightfield photos showed different morphologies of clusters (upper panel, yellow scale bar =100 μm). The hollow cysts prevalent in T1D-1 IPC cultures, which collapse upon fixation, are insulin-negative (column 1). Insulin appears in compact cell clusters rarely found in T1D-1 cultures (column 2) and more predominantly in the ND cultures (column 3). Controls for staining of Insulin (green) were iPS cells (not shown) and cadaveric human islets (column 4). Red color shows DAPI staining. Scale bar = 50 μm.
E) Comparison of the ND and T1D-1 cultures revealed significant disparities in the yield of these two cluster morphologies. Similar to fetal development of the pancreas, we observed in both cases the presence of hollow vacuoles and tight spheroids. However, cells from the T1D-1 patient consisted of significantly more hollow vacuoles than the cells from the ND patient, which had a nearly 50:50 mix of hollow cysts and compact spheroids (n = 3 differentiations for ND cells and 8 for T1D-1 cells). Thus, T1D-1 iPS cells give rise to mostly hollow cyst-like clusters whereas ND iPS cells give rise to a mixture of hollow cysts and compact spheroids. Data are represented as mean ± SEM, **p < 0.01.

Figure 2. IPCs derived from T1D iPS cells poorly express Pdx1 and insulin.
A) To investigate why the T1D cells poorly differentiated into IPCs, mRNA levels of various pancreatic genes were quantified in ND IPCs and T1D-1 IPCs. *Insulin* expression in Stage 5 was accompanied by a striking decrease in *Glucagon* expression in the ND differentiating cultures. However, the T1D-1 culture expressed significantly lower levels of *Insulin* and *Glucagon* compared to ND IPCs. Pdx1 expression in the T1D-1 IPCs was significantly lower than in the ND IPCs ($n = 5$). These data were generated by normalizing Ct values to an iPS cell line. The internal control used in this experiment was the TATA Binding Protein (TBP), which was used as a housekeeping gene. Data are represented as mean ± SEM, $*p < 0.05$, $**p < 0.01$, $***p < 0.001$.
B) 50.5% of the ND IPCs are positive for insulin compared to only 15.9% of T1D-1 IPCs. The flow analysis was repeated 4 times for each cell line.
C) To confirm that those low doses of 5-aza-DC would still demethylate cells, we performed a dot blot for 5-methylcytosine on genomic DNA isolated from untreated T1D-1 iPS cells or iPS cells that were treated with 1 nM or 10 nM 5-Aza-DC (n = 3). Untreated iPS cells possessed significant 5-methylcytosine content (leftmost column), evidenced by the dark spot where the DNA was blotted. As can be observed by lightening of the spots at the 1 nM and 10 nM doses, 5-Aza-DC appeared to effectively demethylate the cells (1 minute represents the exposure time for the blot).

Figure 3. Demethylation of T1D DE cells and not ND DE cells on D4 of differentiation significantly improves the yield of $Pdx1^+$ and $Nkx6.1^+$ cells.
A) In order to identify the optimal time point at which demethylation should be initiated, we established two parallel differentiations of T1D-1 iPS cells into DE cells. In one differentiation, the culture was exposed to 5-Aza-DC on day 0 (which is the day that DE differentiation is initiated), whereas the other culture was demethylated at day 4 of differentiation (which is the last day of DE culture). At the end of the differentiations, we determined the efficacy of DE cell differentiation by studying the expression of CXCR4, PDGFR-α, and Sox17. Undifferentiated T1D-1 iPS cells (red plot) served as a negative control for all of these cell markers. Demethylation of the cells on day 0 of differentiation (green plot) resulted in cells that were $CXCR4^+$ PDGFR-α^+ $Sox17^-$, which represents the immature mesodermal state. In contrast, demethylation of the cells on day 4 (blue plot) generated >90% $CXCR4^+$ $Sox17^+$ PDGFR-α^- cells, representing true DE cells (T1D-2 iPSC data was not shown). This result motivated us to implement demethylation at the end of Stage 1 (on day 4), after generating DE cells, since demethylation at an earlier time point compromised the yield of DE cells. Thus, precise temporal control of the demethylation treatment is necessary to ensure optimal differentiation outcomes.
B) Typically, T1D iPS cells give rise to a disorganized mix of cysts and spheroids (bottom half of leftmost column), with a dominant presence of hollow cysts. Treatment of DE cells with 5-Aza-DC

promotes the formation of compact clusters that uniquely resemble human islets in both size and morphology. Dithizone staining (n = 4) reveals the strong red color of the compact clusters found in the 5-Aza-DC treated cultures, which is reminiscent of islets. This is in contrast to what is observed in the untreated T1D IPC cultures, which stain brown in a manner similar to undifferentiated iPS cells. Black scale bar=100 μm, white scale bar = 50 μm.
C) At the end of Stage 4, the yield of $Pdx1^+$ pancreatic progenitor cells from T1D-1 iPS cells was poor (~12%), which translated into the impaired differentiation of the cells into insulin-expressing cells at the end of Stage 5. To address whether demethylation enhances the yield of $Pdx1^+$ cells from ND iPS cells, we established, in parallel, differentiations of ND iPS cells, treated with or without 10 nM 5-Aza-DC for 18h on day 4 of differentiation .Demethylation of T1D-1 DE cells corrected this impairment and resulted in >95% $Pdx1^+$ cells at the end of Stage 4 (n = 4). However, the yield of $Pdx1^+$ cells was not significantly different between untreated and 5-Aza-DC treated ND IPC cultures. Thus, demethylation enhances the differentiation into IPCs of specifically T1D iPS cells but not ND iPS cells. Undifferentiated iPS cells served as a negative control, whereas the βTC3 mouse insulinoma cell line served as a positive control.
D) Demethylation of T1D-1 DE cells resulted in >95% $Pdx1^+$ cells at the end of Stage 4 (n = 4). A significant proportion of the $Pdx1^+$ cells at the end of Stage 4 co-expressed the pancreatic β-cell specific transcription factor Nkx6.1 (n = 3). Undifferentiated iPS cells served as a negative control.

Figure 4. Demethylation of T1D DE cells yields 50% insulin-expressing cells while averting the generation of glucagon-expressing cells.
A) Whereas untreated T1D iPS cells only yielded up to 1-13.7% $insulin^+$ cells, in cultures treated with 5-Aza-DC, up to 56.7-59.4% of the cells were insulin-expressing (n = 5).
B) At the end of Stage 5, the yield of $Insulin^+$ cells from ND iPS cells was 25%, and this yield did not change after treatment with 5-Aza-DC.
C) The greater emergence of insulin-expressing cells in the 5-Aza-DC treated cultures was accompanied by a drastic decline in the number of glucagon-expressing cells in a concentration-dependent manner (n = 3).
D) A pooled representation from multiple experiments of the yield of $insulin^+$ cells from untreated (n = 3) and demethylated (n = 5) T1D-1 DE cells shows that 5-Aza-DC treatment consistently and significantly augments the yield of IPCs by nearly 4-fold, ***$p < 0.001$. Data are represented as mean ± SEM.

Figure 5. T1D IPCs possess insulin granules and are glucose-responsive.
A) iPS and ES cells typically give rise to a multihormonal pool of precursor cells that only acquire maturity and monohormonal expression of insulin after transplantation in mice. After utilizing 5-aza-DC to generate islet-like compact clusters, we sought to characterize the expression of insulin and glucagon within these cell clusters (n = 4). Consistent with the flow cytometry data, 5-aza-DC appears to promote the generation of unihormonal insulin-expressing cells while averting the formation of glucagon-producing cells. Human islets possess both insulin-expressing and glucagon-expressing cells. Scale bar = 50 μm.
B) IPCs stain positive for cytoplasmic C-peptide, confirming *de novo* production of insulin, and express Nkx6.1 in the nucleus. Tricolor merge on top left and two-color combinations are shown in the other panels. Scale bar = 10 μm.
C) Human islets (left panel) possess insulin granules of various maturities that are differentiated by the color and shape of the core granule. Mature angular insulin granule (□), Maturing round insulin granule (□), and Early round grey insulin granule (□) are identified by the electron microscopy (4000x). However, all granules possess a characteristic "halo" surrounding them, which is very specific to the insulin granule. Similar to islets, T1D-1 IPCs protocol (right panel) possess insulin granules of various maturities, confirming their authenticity and similarity to human islets (n = 3 experiments).
D) Comparison of the number of granules per cell in islets and IPCs reveals a nonsignificant difference between the two cell types. Data are represented as mean ± SEM, n = 57 IPCs and 28 islet pancreatic β-cells counted.

E) After baseline equilibration in 2.8 mM glucose solution (low glucose or LG), exposure to 28 mM glucose (high glucose or HG) resulted in significant increase in insulin secretion by both IPCs and islets **(F).** The fold-increase in insulin secretion **(G)** is higher for IPCs than for islets, $n = 4$ (two experiments of duplicates), $^{**}p < 0.01$, $^{***}p < 0.001$, $^{****}p < 0.0001$. The variation in cell numbers across the cell batches was normalized by total protein content per well.

Figure 6. T1D IPCs rapidly correct hyperglycemia in diabetic mice.
A) STZ-induced diabetic mice (blood glucose levels of ≥300 mg/dL) show rapid correction of hyperglycemia after transplantation with IPCs ($n = 8$). All of the mice show complete and consistent normalization of blood glucose levels within 28 days of IPCs transplant.
B) When subjected to supraphysiological glucose challenge, T1D IPCs-injected mice (showing 5 weeks of stable correction) show effective management of the glucose bolus (2 mg/kg i.p.) by recovering to the baseline normoglycemic state within 4 hours. In contrast, nontransplanted diabetic mice do not recover from severe hyperglycemia. Nondiabetic mice recover to normoglycemia more quickly than IPC-transplanted mice.

Figure 7. T1D IPCs form organoids that express insulin post transplantation.
A) Vascularized tissue derived from the T1D iPS cell-derived IPCs 8 weeks post-transplantation reveals the presence of an organoid-like structure.
B) H&E staining shows glandular morphology of the cells and pancreatic beta cells similar to cadaveric beta cells. Additionally, we observed the presence of duct-like lumens (marked by yellow arrowheads) around which the cells were organized. Image scale bar = 50 μm.
C) Immunofluorescence analysis of cryo-embedded sections of this organoid reveals the presence of insulin-expressing cells that do not express glucagon (gray) or somatostatin (red), **d)** whereas on another section of the organoid, both insulin-expressing (green) and somatostatin-expressing cells were detected. Scale bar = 50 μm.

Figure 1

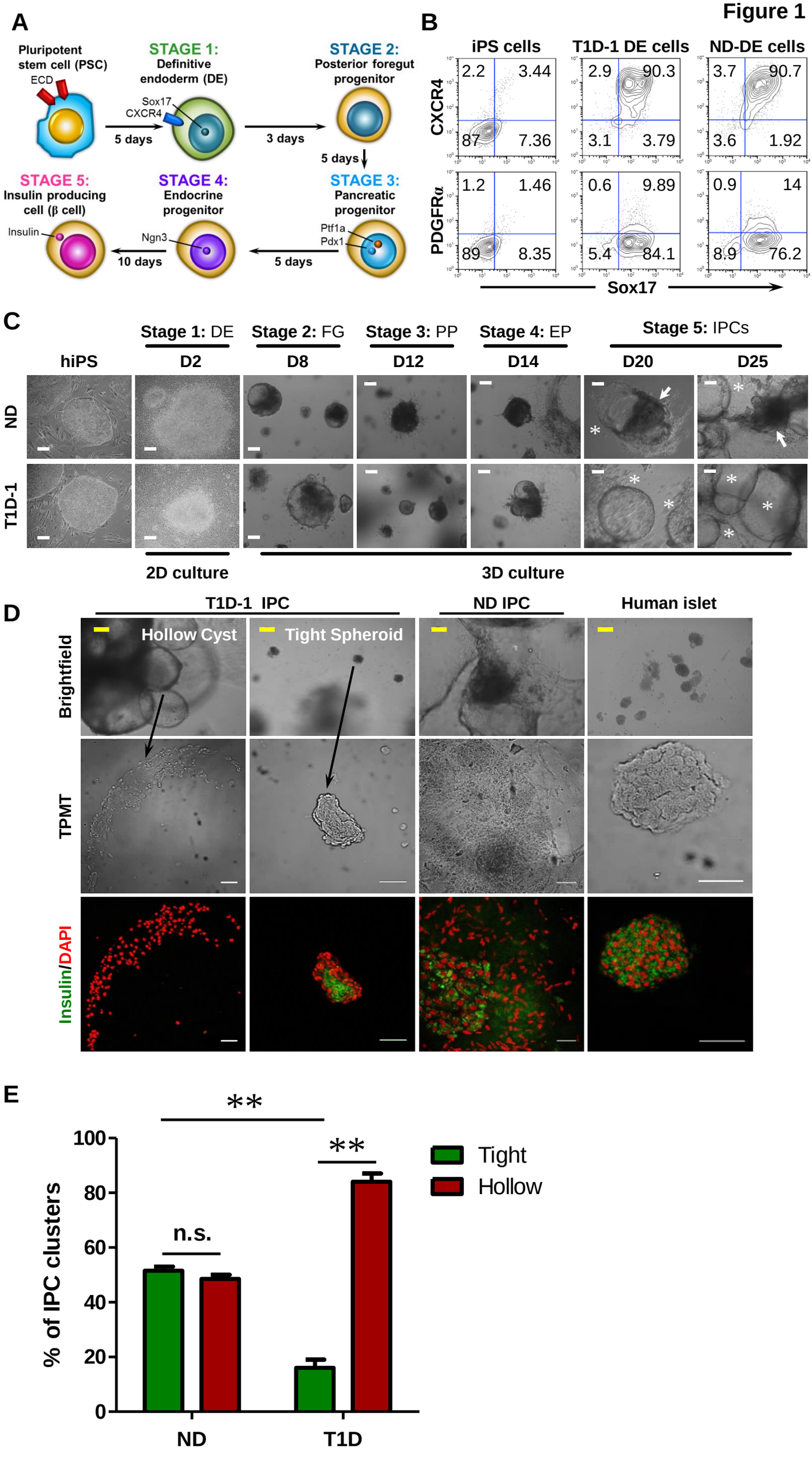
A
Pluripotent stem cell (PSC)
ECD
STAGE 1: Definitive endoderm (DE)
Sox17
CXCR4
5 days
STAGE 2: Posterior foregut progenitor
3 days
5 days
STAGE 3: Pancreatic progenitor
Ptf1a
Pdx1
5 days
STAGE 4: Endocrine progenitor
Ngn3
10 days
STAGE 5: Insulin producing cell (β cell)
Insulin
B
iPS cells
T1D-1 DE cells
ND-DE cells
CXCR4
PDGFRα
2.2
3.44
87
7.36
2.9
90.3
3.1
3.79
3.7
90.7
3.6
1.92
1.2
1.46
89
8.35
0.6
9.89
5.4
84.1
0.9
14
8.9
76.2
Sox17
C
Stage 1: DE
Stage 2: FG
Stage 3: PP
Stage 4: EP
Stage 5: IPCs
hiPS
D2
D8
D12
D14
D20
D25
ND
T1D-1
2D culture
3D culture
D
T1D-1 IPC
ND IPC
Human islet
Hollow Cyst
Tight Spheroid
Brightfield
TPMT
Insulin/DAPI
E
**
**
n.s.
100
80
60
40
20
0
% of IPC clusters
ND
T1D
Tight
Hollow

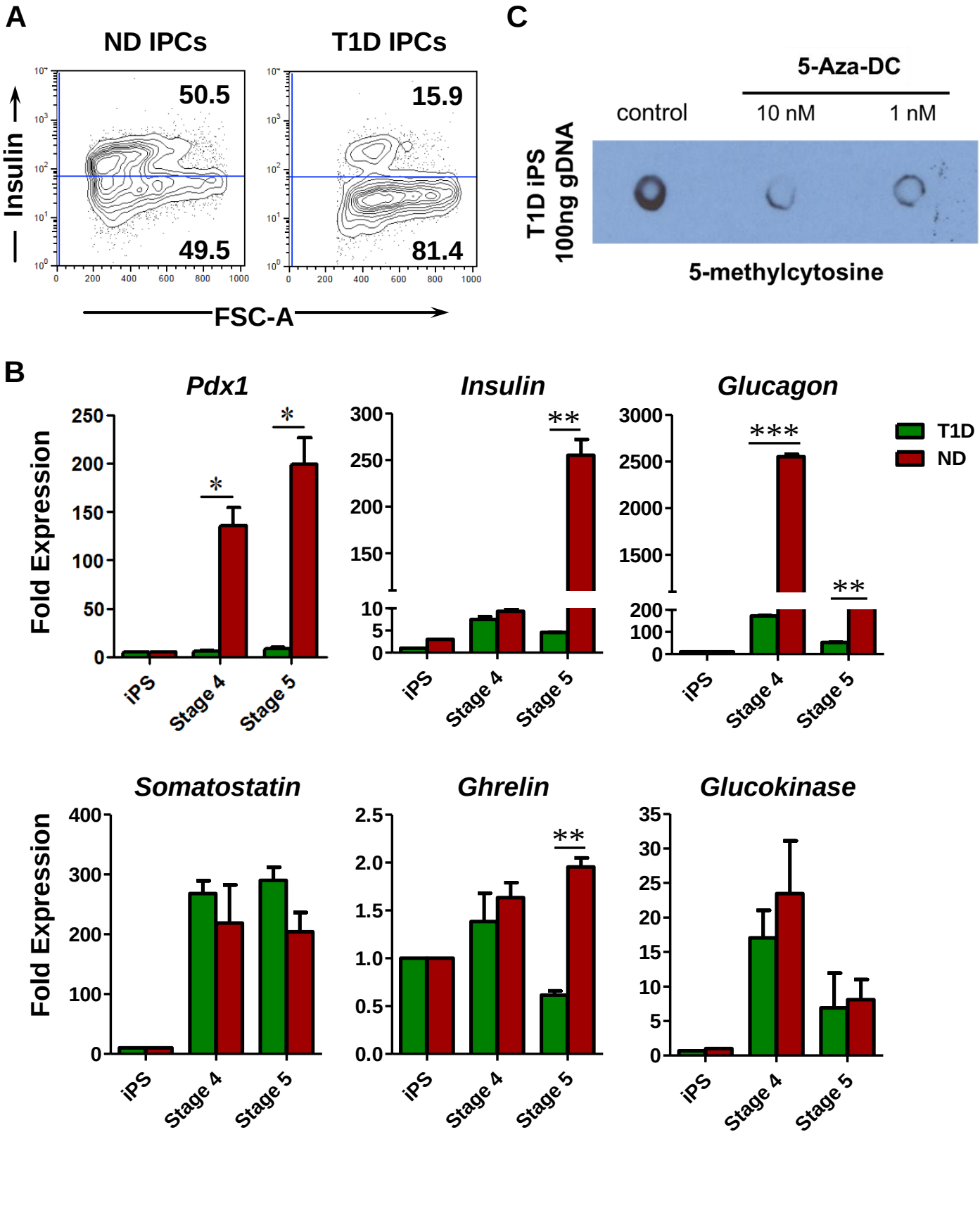
A
ND IPCs
T1D IPCs
50.5
49.5
15.9
81.4
Insulin
FSC-A
C
5-Aza-DC
control
10 nM
1 nM
T1D iPS
100ng gDNA
5-methylcytosine
B
Pdx1
Insulin
Glucagon
Somatostatin
Ghrelin
Glucokinase
Fold Expression
T1D
ND
iPS
Stage 4
Stage 5

Figure 3

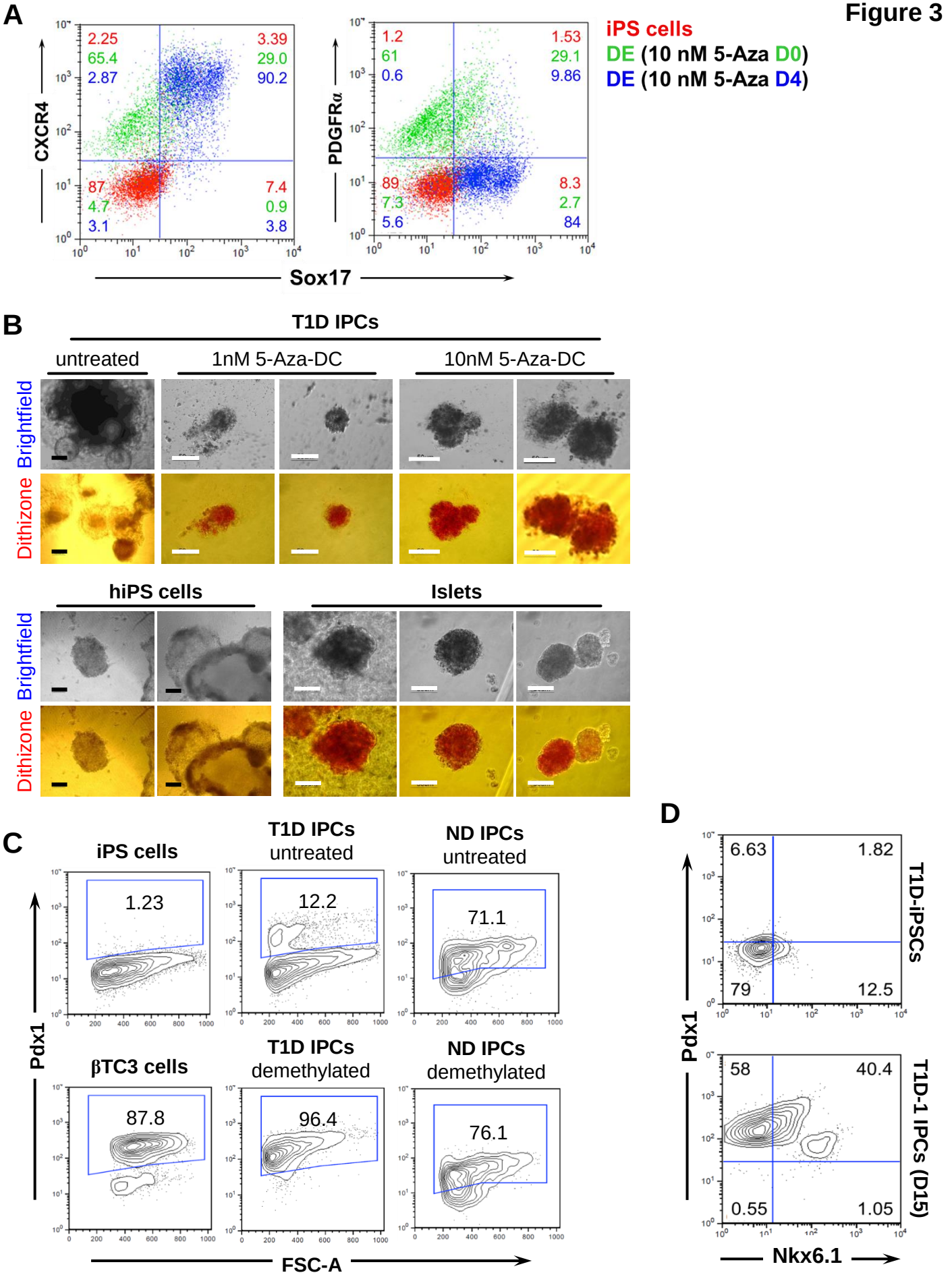
A
iPS cells
DE (10 nM 5-Aza D0)
DE (10 nM 5-Aza D4)
CXCR4
PDGFRα
Sox17
2.25
65.4
2.87
3.39
29.0
90.2
87
4.7
3.1
7.4
0.9
3.8
1.2
61
0.6
1.53
29.1
9.86
89
7.3
5.6
8.3
2.7
84
B
T1D IPCs
untreated
1nM 5-Aza-DC
10nM 5-Aza-DC
Brightfield
Dithizone
hiPS cells
Islets
C
iPS cells
T1D IPCs untreated
ND IPCs untreated
βTC3 cells
T1D IPCs demethylated
ND IPCs demethylated
Pdx1
FSC-A
1.23
12.2
71.1
87.8
96.4
76.1
D
T1D-iPSCs
T1D-1 IPCs (D15)
Pdx1
Nkx6.1
6.63
1.82
79
12.5
58
40.4
0.55
1.05

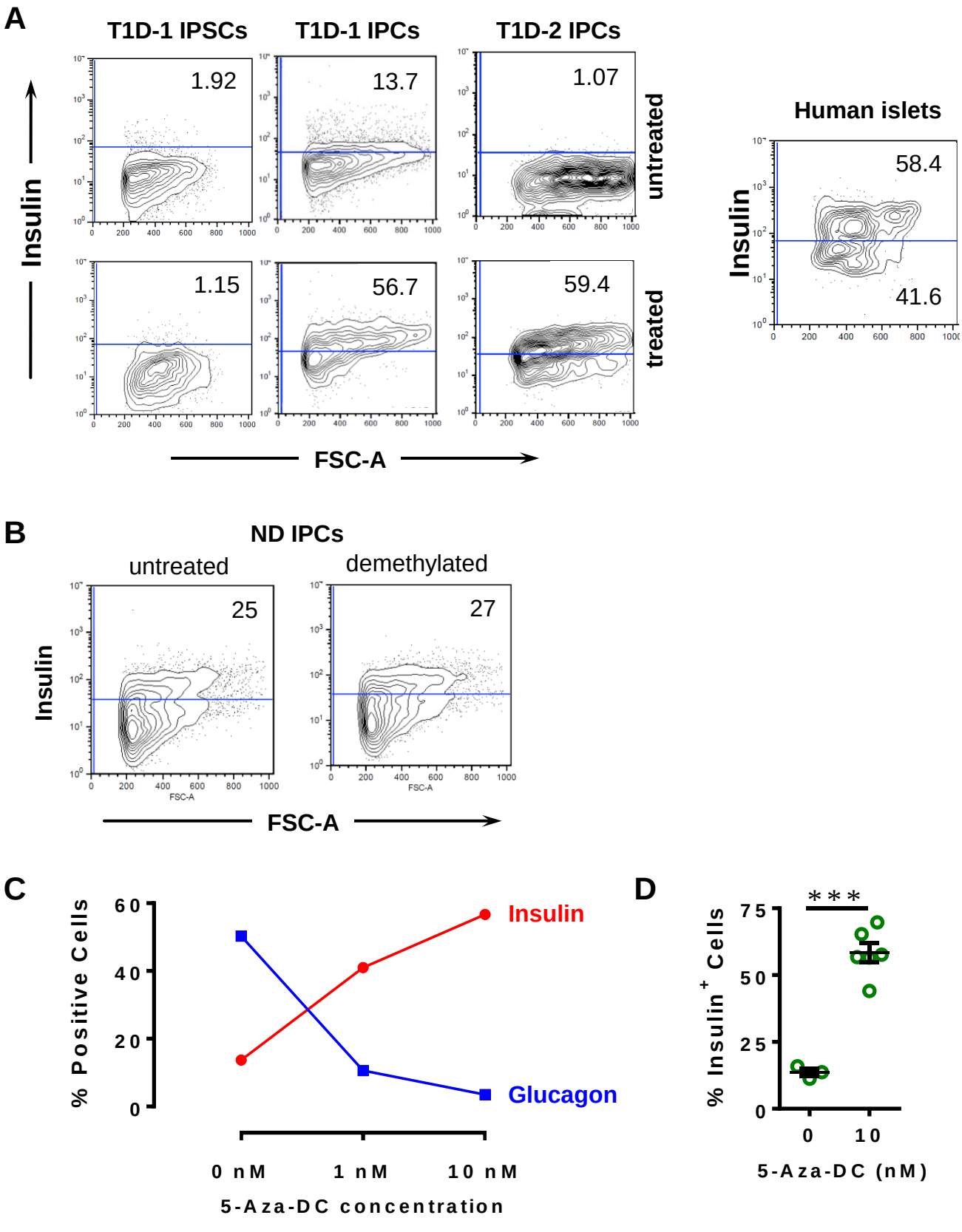
A
T1D-1 IPSCs
T1D-1 IPCs
T1D-2 IPCs
1.92
13.7
1.07
untreated
1.15
56.7
59.4
treated
Insulin
FSC-A
Human islets
58.4
41.6
B
ND IPCs
untreated
demethylated
25
27
Insulin
FSC-A
C
% Positive Cells
Insulin
Glucagon
0 nM
1 nM
10 nM
5-Aza-DC concentration
D
% Insulin+ Cells
***
5-Aza-DC (nM)

Figure 5

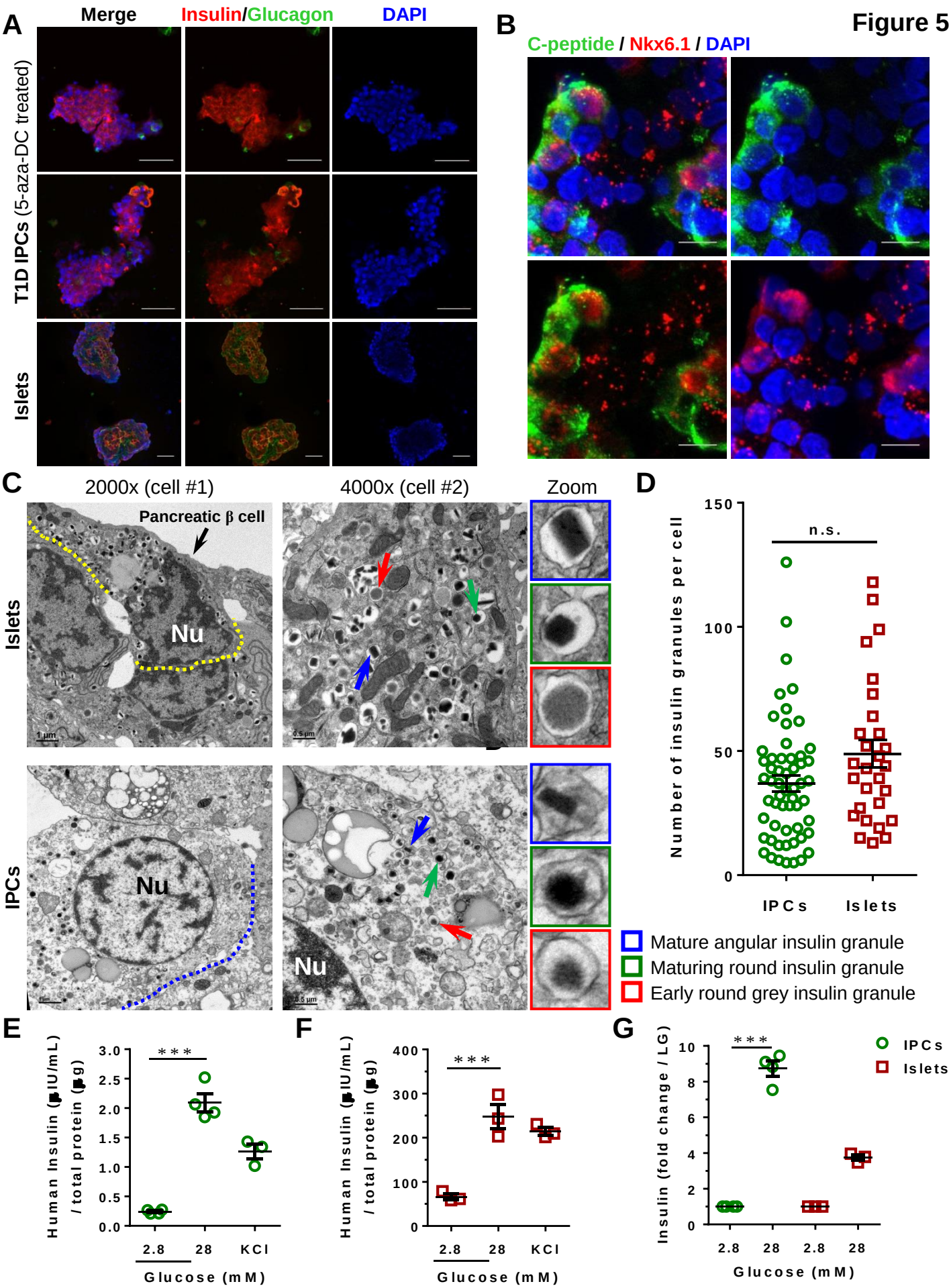
A
Merge
Insulin/Glucagon
DAPI
T1D IPCs (5-aza-DC treated)
Islets
B
C-peptide / Nkx6.1 / DAPI
C
2000x (cell #1)
4000x (cell #2)
Zoom
Islets
IPCs
Pancreatic β cell
Nu
D
Number of insulin granules per cell
n.s.
IPCs
Islets
Mature angular insulin granule
Maturing round insulin granule
Early round grey insulin granule
E
Human Insulin (μIU/mL) / total protein (μg)
***
2.8
28
KCl
Glucose (mM)
F
Human Insulin (μIU/mL) / total protein (μg)
***
2.8
28
KCl
Glucose (mM)
G
Insulin (fold change / LG)
***
IPCs
Islets
2.8
28
2.8
28
Glucose (mM)

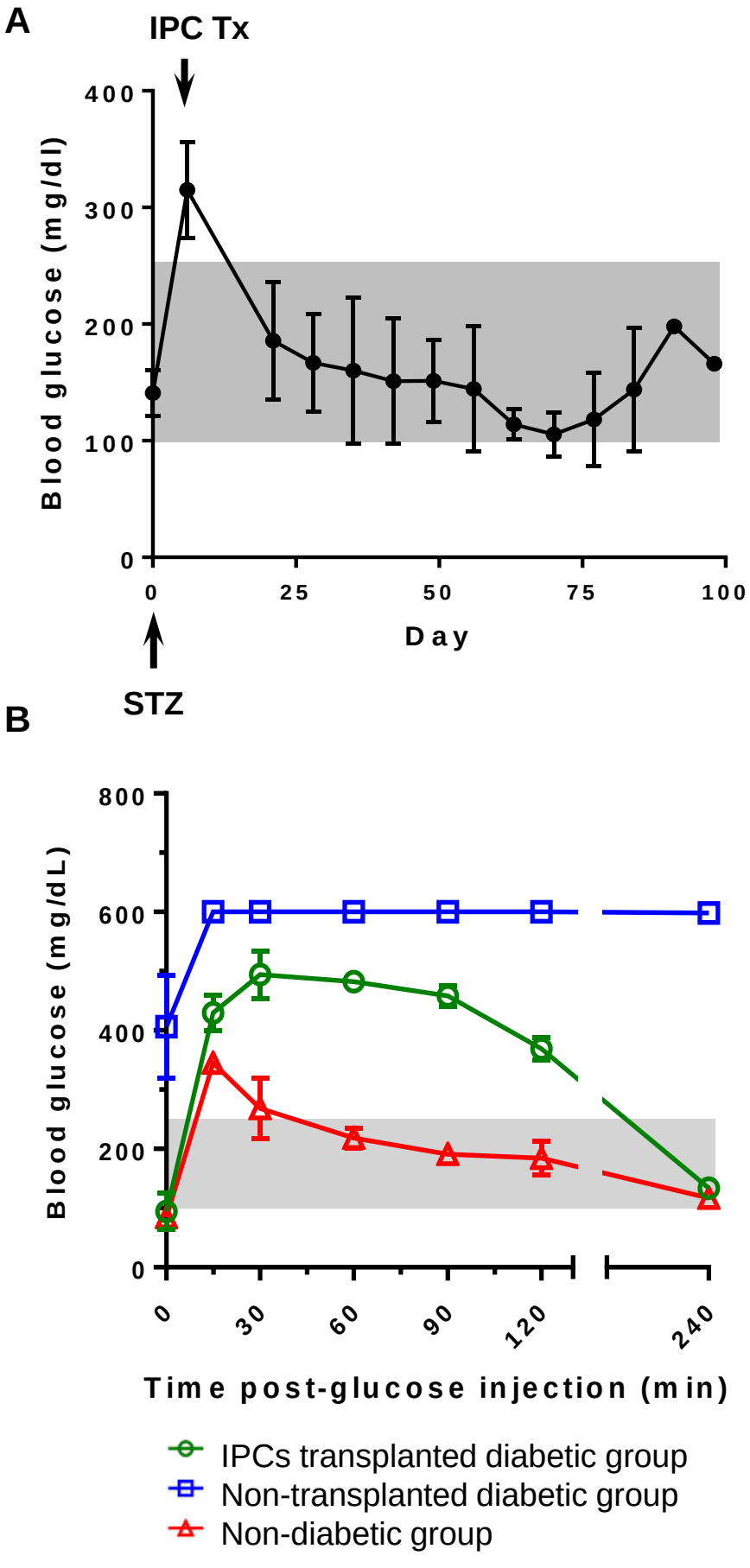
A
IPC Tx
Blood glucose (mg/dl)
400
300
200
100
0
0
25
50
75
100
Day
STZ
B
Blood glucose (mg/dL)
800
600
400
200
0
0
30
60
90
120
240
Time post-glucose injection (min)
IPCs transplanted diabetic group
Non-transplanted diabetic group
Non-diabetic group

Figure 7

Insulin / Glucagon / Somatostatin / DAPI

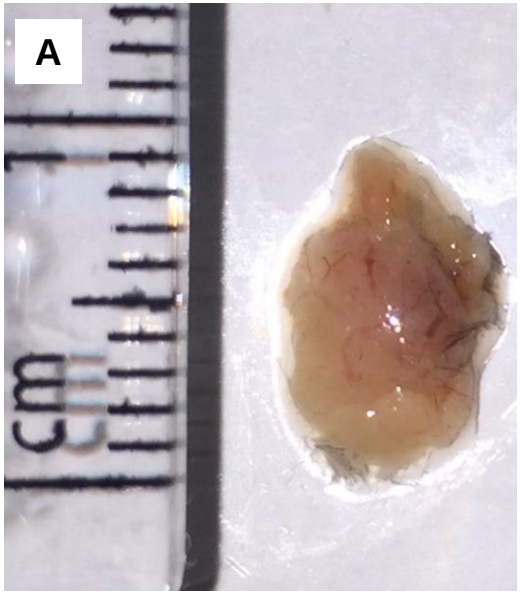

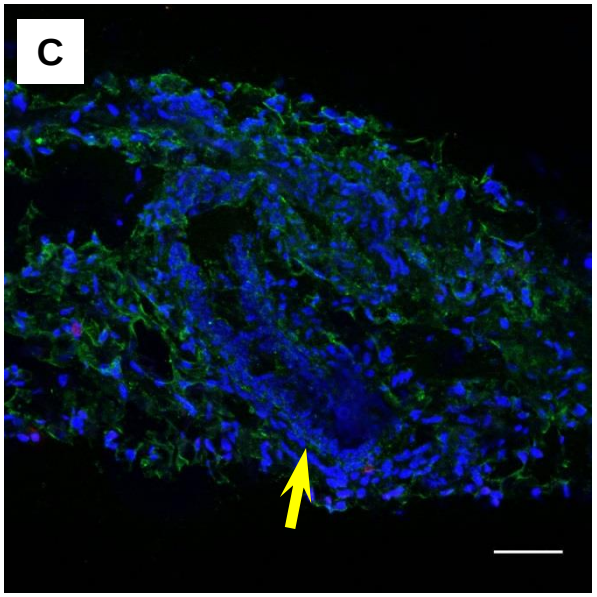

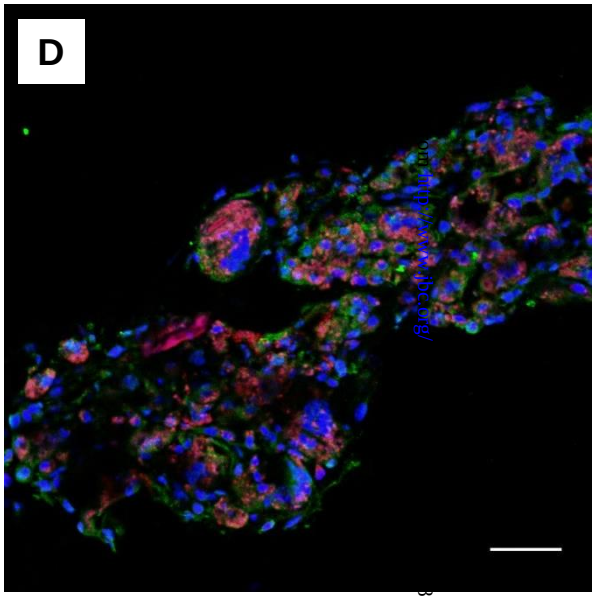

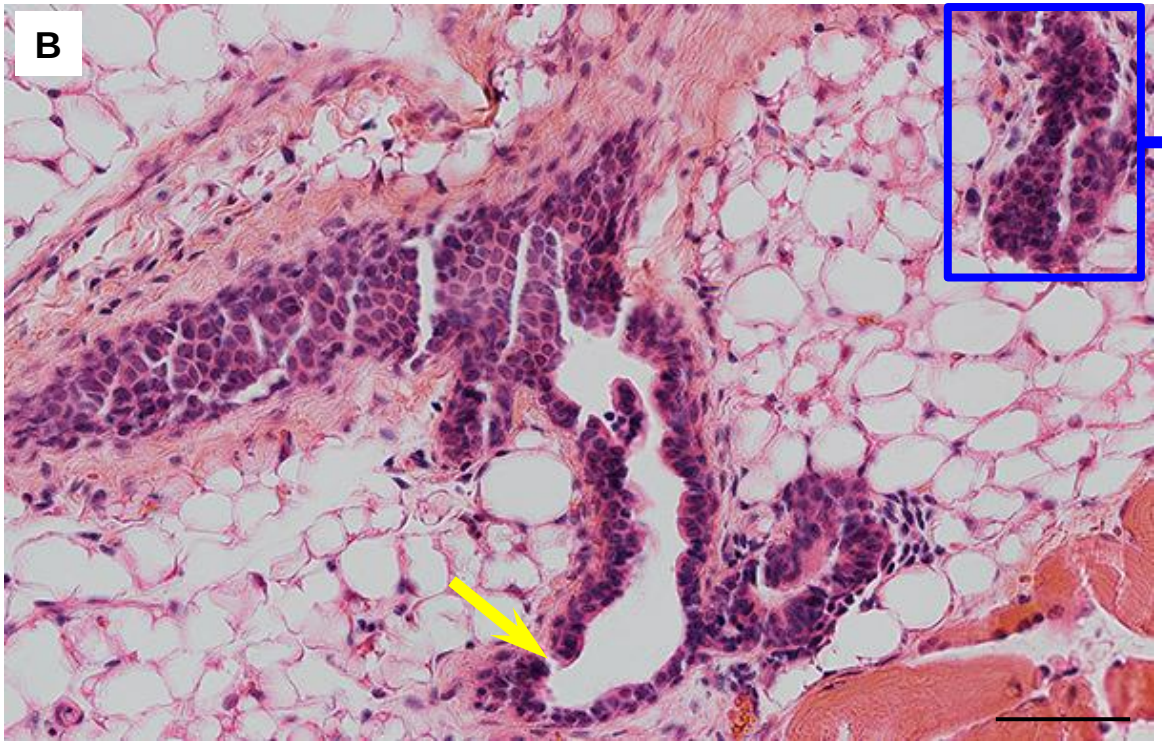

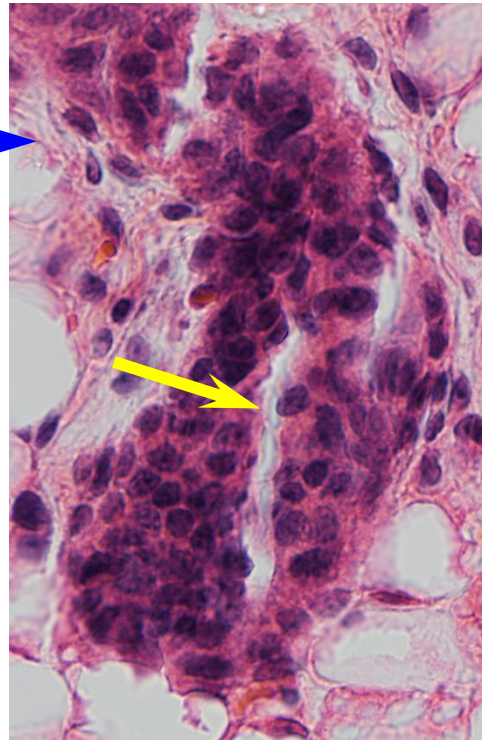

Demethylation of Induced Pluripotent Stem Cells from Type 1 Diabetic Patients Enhances Differentiation into Functional Pancreatic β-cells

Gohar S. Manzar, Eun-Mi Kim and Nicholas Zavazava

J. Biol. Chem. published online March 30, 2017

Access the most updated version of this article at doi: 10.1074/jbc.M117.784280